

Notice: This manuscript has been coauthored by UT-Battelle, LLC, under Contract No. DE-AC0500OR22725 with the U.S. Department of Energy. The United States Government retains and the publisher, by accepting the article for publication, acknowledges that the United States Government retains a non-exclusive, paid-up, irrevocable, world-wide license to publish or reproduce the published form of this manuscript, or allow others to do so, for the United States Government purposes. The Department of Energy will provide public access to these results of federally sponsored research in accordance with the DOE Public Access Plan (<http://energy.gov/downloads/doe-public-access-plan>).

Inversion of Dislocation-Impurity Interactions in α -Fe under Magnetic State Changes

Franco Moitzi,¹ Lorenz Romaner,² Andrei V. Ruban,^{1,3} Swarnava Ghosh,⁴ Markus Eisenbach,⁴ and Oleg E. Peil¹

¹*Materials Center Leoben Forschung GmbH, Roseggerstraße 12, A-8700 Leoben, Austria*

²*Chair of Physical Metallurgy and Metallic Materials, Department of Materials Science, University of Leoben, Roseggerstraße 12, A-8700 Leoben, Austria*

³*Department of Materials Science and Engineering, Royal Institute of Technology, 10044 Stockholm, Sweden*

⁴*National Center for Computational Science, Oak Ridge National Laboratory, Oak Ridge, Tennessee 37831, USA*

(Dated: December 20, 2024)

Impurities can strongly influence dislocation behavior and thus impact plasticity. Quantifying dislocation-impurity interactions in α -Fe from *ab initio* across a wide temperature range is challenging due to paramagnetism at elevated temperatures.

In this work, we investigate the energy profiles and segregation behavior of various *3d* elements—V, Cr, Mn, Cu, Ni, and Co—in and around $1/2\langle 111 \rangle$ screw dislocations in α -Fe in ferromagnetic and paramagnetic state with the latter being modeled through both the disordered local moment model and a spin-wave approach using *ab initio* methods. Our findings reveal that (1) magnetic effects are large compared to elastic size effects, and (2) dislocation-impurity interactions are dependent on the magnetic state of the matrix and thermal lattice expansion. In particular, Cu changes from core-attractive in the ferromagnetic state to repulsive in the paramagnetic state.

Plastic deformation in metallic materials is largely governed by the creation, motion, and interaction of dislocations with impurities and other defects. Among these mechanisms, dislocation-impurity interactions play a key role. By alloying, one can control the type and amount of impurities and potentially fine-tune the material's properties. This is particularly relevant in body-centered cubic (bcc) alloys, which exhibit complex dislocation phenomena compared to face-centered cubic (fcc) alloys [1, 2]. At moderate temperatures, the deformation in such alloys is dominated by screw dislocations, which move through a thermally activated process involving kink-pair nucleation and propagation [3, 4]. Despite this complexity, important trends in yield strength can be predicted based on the behavior of isolated $1/2\langle 111 \rangle$ screw dislocations in pure bcc metals [5, 6] or bcc alloys [7–11].

Among those bcc materials, α -Fe in the form of ferritic steel holds substantial technological importance [12]. *Ab initio* description of this material is challenging due to the complex magnetic states, which include ferromagnetism (FM) at low temperatures and paramagnetism (PM) above the Curie-Temperature T_C in the form of disordered moments.

At the dislocation core, the interaction between local atomic coordination, volumetric changes, and magnetic coupling exerts a significant influence on interatomic interactions, which can be seen from the different magnetic moments at the core [8, 13–16]. This phenomenon is particularly relevant when describing the strengthening ef-

fect of impurities, which arises due to their impact on the energy barriers that dislocations must overcome to unpin and glide. Alloying α -Fe with other *3d* magnetic elements introduces additional complex interactions that cannot be fully explained by elastic size mismatches alone, complicating the application of simpler models [17–19].

Only a few *ab initio* studies have investigated the energy profiles of magnetic impurity around dislocation cores [10, 11], with the latter also examining the influence of the PM states on energy profiles. These studies only focused on Ni and Cr, and as a result, they did not discover impurities displaying altered segregation behavior with increasing temperature.

In the present study, we investigate from first principles the impact of a broader range of *3d*-element impurities (V, Cr, Mn, Cu, Ni, and Co) and magnetic states on $1/2\langle 111 \rangle$ screw dislocations in α -Fe alloys. We find that for almost all elements in question, the interaction energy changes sign when going from the low-temperature (FM) to high-temperature (PM) state, with the strongest effect being observed for Cu. To check the robustness of our results, we employ several different density-functional theory (DFT) methodologies and two methods for treating the PM state. Furthermore, we test energy variations due to the choice of the exchange-correlation (XC) functional and the account of lattice relaxations.

Calculations are performed using the Vienna Ab-initio Simulation Package (VASP) [20–22] with semicore *p*-states included as valence states [23, 24], the Exact Muffin-Tin Orbital (EMTO) method with full-charge

density formalism [25, 26] (Lyngby version [27])—which combines Green’s function-based DFT with the coherent potential approximation (CPA) for total energy computations—and the EMTO-based Locally Self-Consistent Green’s Function (ELSGF) technique [28, 29]. Green’s function methods enable disordered local moment (DLM) approximation for describing the PM state. As an alternative to DLM, we also use the Locally-Self Consistent Multiple Scattering (LSMS) code [30–32] for carrying out spin-wave method (SWM) [33] calculations, which requires large supercells. The dislocations are modeled with the dipole approach [34] with a 135 atoms base. Effects of thermal expansion are taken into account by considering two lattice constants: $a_{LT} = 2.8341 \text{ \AA}$ for low T (LT) and $a_{HT} = 2.8893 \text{ \AA}$ for 973 K (HT), the latter temperature being just below the Curie temperature of 1043 K. Unless specified otherwise, the calculations are done with the local density approximation (LDA) exchange-correlation (XC) functional in the Perdew-Wang parametrization [35]. The motivation for this choice is provided further in the text when we discuss differences between results within LDA and generalized gradient approximation (GGA).

We characterize the dislocation-impurity interaction strength by evaluating the energy of the segregation to the core, taken as the difference between the energy at a core site and a reference site in the bulk, $E_{\text{seg}} = E_{X \rightarrow \text{Fe}}^{\text{core}} - E_{X \rightarrow \text{Fe}}^{\text{bulk}}$, where $X \rightarrow \text{Fe}$ denotes an impurity X substituted at Fe site.

This quantity reflects the ability of an element X to pin a dislocation. For core sites, we select one of the three equivalent positions surrounding the screw dislocation core (first shell in the differential displacement map marked by a triangle Fig. 4), while the reference site, positioned as far as possible from the core, is located six atomic shells away (rightmost site within the purple box in Fig. 4).

The segregation energies, E_{seg} , calculated with ELSGF in both FM and PM states for six different impurities (V, Cr, Mn, Co, Ni, Cu) and for the two lattice constants are presented in Fig. 1a. One can see very distinct trends in different magnetic states. In the FM state at the LT lattice constant, V, Cr, and Co exhibit positive segregation energies close to zero, implying weak attraction to the dislocation core. In contrast, Mn, Ni, and especially Cu have a strong tendency to segregate to the core. Furthermore, changing from the LT to the HT value of the lattice constant does not change the overall trend, but just shifts the energies upward (toward more repulsive values) by a constant value of $\sim 0.08 \text{ eV}$. As to the PM state, it is characterized by only a marginal volume effect on E_{seg} , with V, Cr, and Co having energies similar to their counterparts at a_{LT} in the FM state. The three other elements, Mn, Ni, and Cu, on the other hand, demonstrate a behavior very different from that in the FM state. Specifically, Mn has nearly zero negative segregation energy, Ni exhibits weak attraction, while Cu becomes a significantly repulsive impurity. Juxtaposing

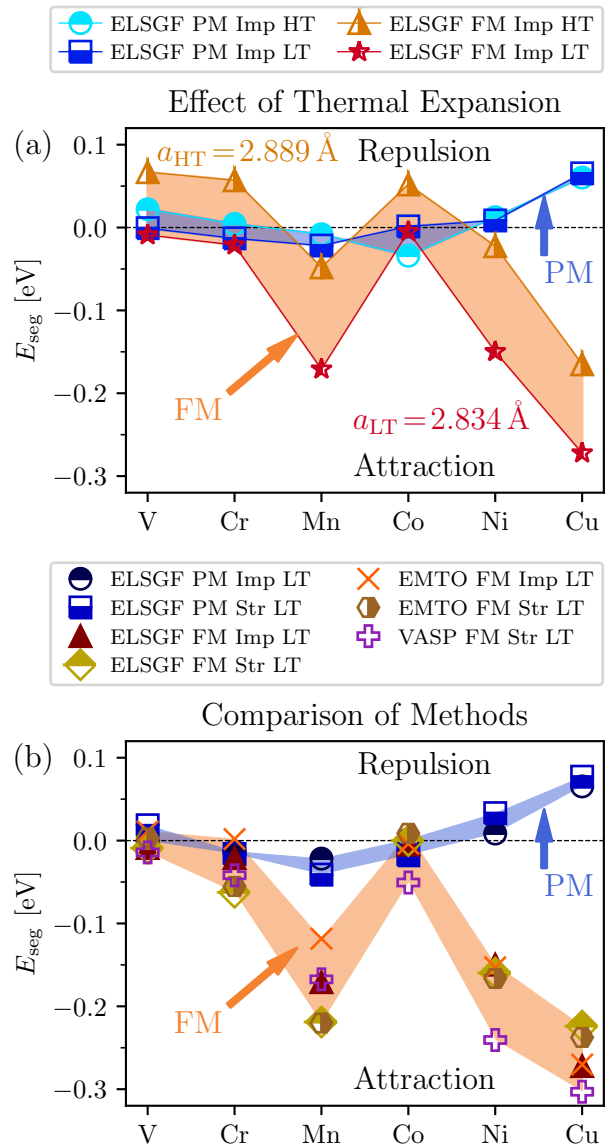


FIG. 1. Segregation energies to the dislocation core site for $3d$ -elements (V, Cr, Mn, Co, Ni, Cu) in bcc Fe. The energies are calculated for both paramagnetic (PM) and ferromagnetic (FM) states using ELSGF, EMTO, and VASP methods. (Str) refers to a string chain of impurities along the z -direction, while (Imp) represents a single impurity atom (dilute limit) surrounded by Fe atoms along the z -direction. (a) effect of thermal expansion by calculating at lattice constant for LT and HT. (b) effect of the specific method and setup.

the most physically relevant cases of the FM state at a_{LT} and the PM state at a_{HT} , we can conclude that most of the elements under consideration—Cr, Co, Ni, Cu—invert the sign of their interaction with the dislocation core. At the same time, although the interaction energy of Mn does not change sign, its absolute value drops dramatically, almost to zero. Only V shows practically no variations with the magnetic state and seems to be af-

fected only by volume.

The two groups of elements, (Mn, Ni, Cu) and (V, Cr, Co), differ in another important aspect of their behavior in different magnetic states. For the first group, the segregation energy at the HT lattice constant goes up when switching from the FM to the PM state, i.e., paramagnetism at high temperature makes them more repulsive. The behavior is opposite for the second group of elements, for which paramagnetism drives them more toward attractive interactions (or, at least, less repulsive). This has implications for the temperature dependence of the segregation energy, as will be discussed later in the text.

The trends described above are also consistent across various impurity configurations and computational methods, as can be seen in Fig. 1b. In particular, we compare two contrasting setups: a chain of impurity atoms along the z-axis (denoted as “Str” in Fig. 1), and a single impurity atom surrounded by Fe atoms along the z-axis (denoted as “Imp”). In the CPA-based EMTO, the latter configuration is modeled as the dilute limit of the Fe-X alloy at a respective site, while in cases of ELSGF and VASP, a 4-layer structure along the z-direction is used. For Mn in the FM state, the difference between different configurations is the largest, due to the sensitivity of the local magnetic moment of Mn to the local atomic configuration. Therefore, the segregation energy—a small quantity overall—is notably affected in this case: EMTO-CPA yields approximately the value of -0.11 eV, while the result for 4-layer ELSGF is -0.16 eV, highlighting the influence of impurity-impurity interactions. However, it is clear from Fig. 1 that neither the differences between the configurations nor the discrepancies between the methods alter the qualitative picture presented in Fig. 1a.

Other potential sources of uncertainty for our results include the choice of the XC functional and the effect of atomic relaxations. Our initial choice of LDA is motivated by its better account of magnetic effects compared to the common generalized gradient approximations (GGA) in the Perdew-Burke-Ernzerhof parametrization [36–39]. At the same time, the well-known LDA error in determining the equilibrium volume is irrelevant in our calculations, as the lattice constant is fixed to experimental values.

The effects of the XC functional and relaxations are shown in Fig. 2, where we present the segregation energies of relaxed and unrelaxed impurity configurations calculated with VASP in the FM state at a_{LT} using LDA and PBE functionals. First, it is worth noting that our PBE values for Ni and Cr align well with those reported in Refs. 10 and 11, even though the latter were obtained with different methods. Compared to LDA results, the segregation energies within PBE are shifted upward, causing V and Cr to switch from weak attraction to weak repulsion. However, despite considerable changes in the energies, the trends remain qualitatively consistent with the ones obtained within LDA. Although one can expect that gradient corrections could improve the

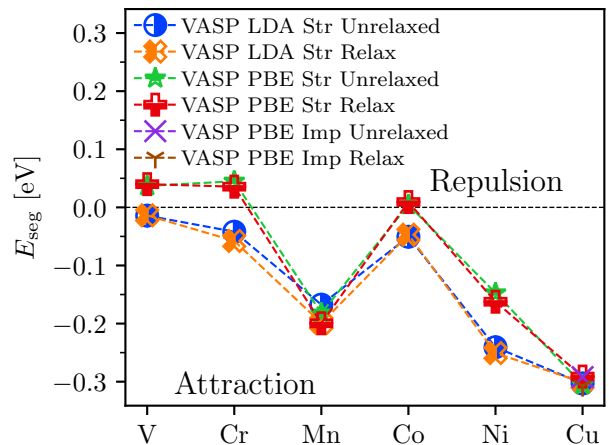


FIG. 2. Comparison of segregation energies of impurities to the dislocation core (E_{seg}) for 3d-elements (V, Cr, Mn, Co, Ni, Cu) in bcc Fe. The segregation energies are evaluated using both PBE and LDA functionals. E_{seg} is shown with and without atomic relaxation (Relax) following impurity introduction. (Str) refers to a string chain of impurities along the z-direction, while (Imp) represents a single impurity atom surrounded by Fe atoms along the z-direction.

energy in the non-centrosymmetric atomic environment inside the core, we can also argue that PBE might bias the results by overestimating magnetic exchange contributions [37–39]. It is therefore difficult to say, which of the two functional gives more accurate results, and we stick to LDA for the reasons set out above.

The effect of relaxations is estimated using VASP by allowing an impurity atomic configuration to relax and comparing the obtained energy to the unrelaxed one. It is important to keep in mind that here we talk only about relaxations after the impurity substitution, the initial core configuration of pure Fe being fully relaxed in the FM state. The equilibrium dislocation structure in the PM state is very similar to that in the FM state, with both exhibiting the easy-core configuration, which was found by via non-colinear DLM [16] and SWM [40] calculations.

As seen in Fig. 2, the relaxation effects are practically negligible for both LDA and PBE, despite the significant lattice distortion around the core in pure Fe. A similar result has already been reported in Ref. 10 for Ni and Cr. The outcome is not unexpected because the size mismatch between Fe and elements under consideration is marginal, and the impurities do not alter the core configuration. Although most of the relaxation tests were done for the string of impurities at the core (denoted as “Str” in Fig. 2), we have additionally checked a single-impurity configuration (the 4-layer setup) for selected elements and found also in this case that the relaxation contributions are insignificant.

To illustrate better a potential impact of the obtained energies on the dislocation-impurity interaction during

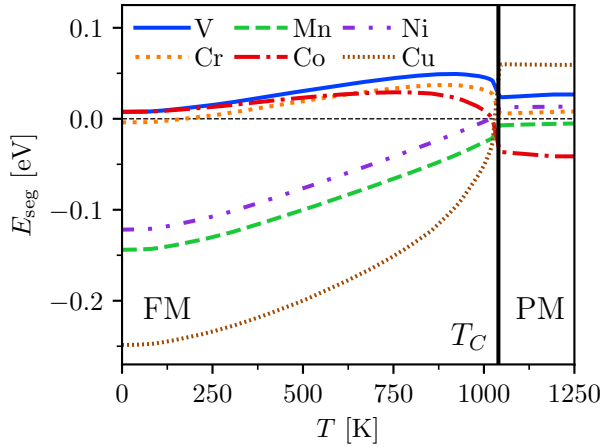


FIG. 3. Segregation energies as a function of temperature from 0 K to Curie temperature at 1043 K obtained by fitting $E_{\text{seg}}(m, a)$ to experimental magnetization $m(T)$ and lattice constant $a(T)$.

heat treatment, let us define the segregation energy as a function, $E_{\text{seg}}(m, a)$, of the reduced magnetization, $m = M/M_s$ —with M being the magnetization at a given temperature and volume, M_s the saturation magnetization at 0 K—and of the lattice parameter, $a = \{a_{\text{LT}}, a_{\text{HT}}\}$. Considering the results in Fig. 1a as four boundary cases with $m = \{0, 1\}$ (corresponding to the FM and PM states, respectively) and $a = \{a_{\text{LT}}, a_{\text{HT}}\}$ for each impurity, we can define $E_{\text{seg}}(m, a)$ as an interpolation within these bounds. We choose the bilinear interpolation as the simplest one, which consistently takes into account that interatomic interactions are coupled to the magnetization [41]. Such a model can be constructed as a linear interpolation for E_{seg} in a , with the coefficients being, in turn, linear functions of m (see Supplemental Materials, SM, for details).

Once the function $E_{\text{seg}}(m, a)$ is determined, we can use experimental values for the lattice constant, $a(T)$ [42], and the reduced magnetization, $m(T)$ [43], as functions of temperature to get $E_{\text{seg}}(T) \equiv E_{\text{seg}}(m(T), a(T))$. The computed temperature-dependent segregation energies for the elements in question are plotted in Fig. 3. The plots for Mn, Ni, and Cu only confirm the conclusions made above. However, the T -dependence of E_{seg} for V, Cr, and Co reveals a non-trivial behavior: Weak segregation/repulsion at LT, followed by an increasing repulsion due to lattice expansion at HT, and finally, segregation energies falling back to small values in the PM state, with Co and Cr exhibiting a weak inversion of the interaction energy. Moreover, this group of elements exhibits a maximum in E_{seg} at some temperature below the Curie temperature. This non-monotonic behavior can be traced back to the positive value of $E_{\text{seg}}(1, a_{\text{HT}}) - E_{\text{seg}}(0, a_{\text{HT}})$ (mentioned earlier), which can be inferred from the properties of function $E_{\text{seg}}(m, a)$, as elaborated in more details in SM.

It is worth pointing out, that the above picture of the

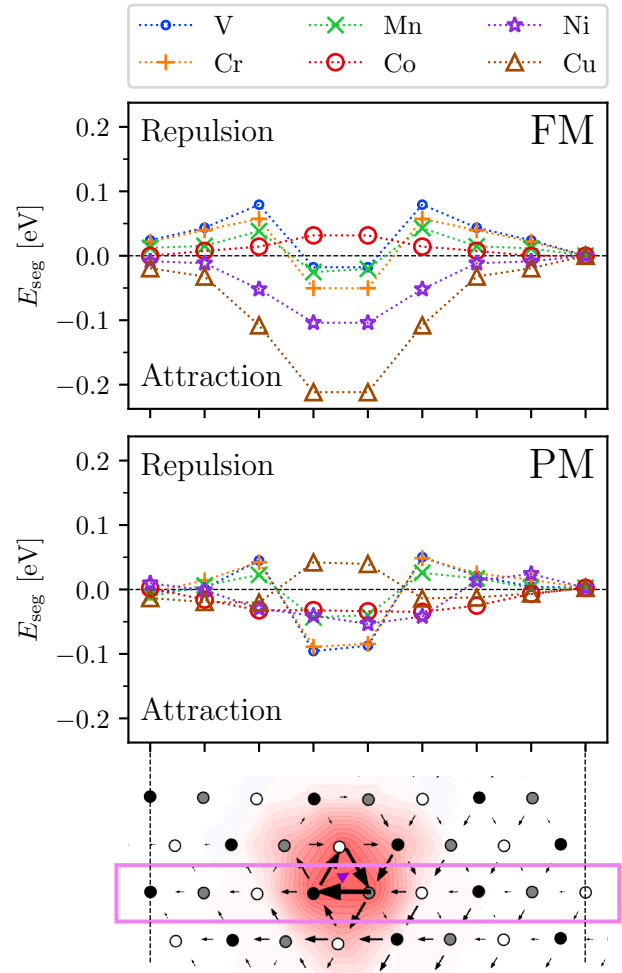


FIG. 4. Energy profile of the segregation energies across the dislocation core for 3d elements (V, Cr, Mn, Co, Ni, Cu) in bcc Fe together with differential displacement maps and nye tensor representation. The energies are calculated for both paramagnetic (PM) and ferromagnetic (FM) states using LSMS for a chain of impurities along the z -direction.

evolution with temperature is only an approximate one, as we use a rather simple model for $E_{\text{seg}}(m, a)$ and neglect other temperature effects, such as, e.g., entropic contributions due to phonons. Nevertheless, we believe that a more precise calculation will not change the major qualitative features.

Thus far, we have considered the segregation energy right to the core site of the dislocation. To study energy profiles in the vicinity of the core, we leverage the efficiency of the LSMS method that can easily handle thousands of atoms, also with non-collinear spin configurations. As DLM is not available in this code, we use as spin-wave method (SWM) [33] as an alternative for modeling of the paramagnetic state. Within the SWM, we approximate the PM state by averaging the total energies over planar spin spiral configurations corresponding to the wave vectors from an 8-point Monkhorst-Pack

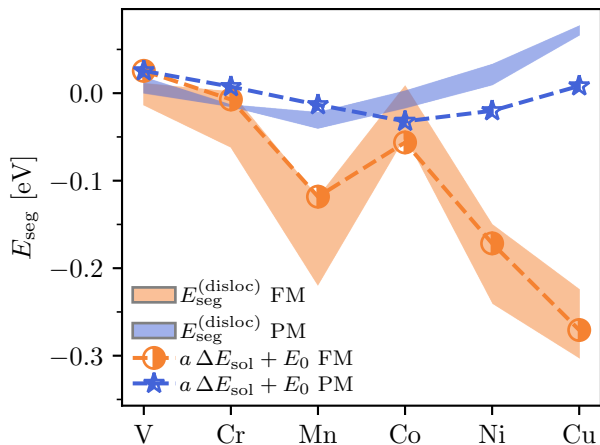


FIG. 5. Lines: Segregation energy model from energy differences between fcc and bcc solution energies for $3d$ -elements (V, Cr, Mn, Co, Ni, Cu) in FM and PM states. Shaded areas: Range of segregation energies using different methods (see also Fig. 1b).

grid.

We consider a symmetric profile along a cut through the dislocation core, intersecting two atomic sites at the dislocation core. The results for the two magnetic states at a_{HT} are presented in Fig. 4, which also includes a differential displacement map and Nye tensor visualization of the corresponding cut through the dislocation structure. First, we would like to note that the obtained segregation energies are consistent with the other methods for all elements except for Mn in the FM state. The reason for this is a magnetically frustrated state of Mn in the string configuration, inherent only to the FM state of Fe. The PM calculations within SWM, on the other hand, give qualitatively similar results as DLM calculations with ELSGF.

Focusing on the shape of energy profiles, we can distinguish two main types: Monotonic (a single hill or a valley at the core, e.g., Co, Ni, Cu in FM-Fe in Fig. 4) and non-monotonic (peaks and valleys, e.g., V, Cr, Mn in FM-Fe Fig. 4). The non-monotonic energy profiles for V, Cr, and Mn do not change when switching from the FM to the PM state. The monotonic profile for Co does not change its shape, but it flips from a repulsive (hill-like) to attractive (valley-like) behavior. The most interesting transformation happens to the profiles of Ni and Cu, whose shape changes from the monotonic one in the FM state to the non-monotonic one in the PM state. While for Ni this effect is weak and can be affected by methodological uncertainties, the result for Cu is rather robust. Apart from a rather strong inversion of the interaction sign for Cu, such non-monotonic changes in the segregation energy in the vicinity of the core might have an impact on the propagation mechanism of dislocations near impurities.

Overall, Cu impurity exhibits the strongest change in

the segregation tendency as a magnetic state evolves from low to high temperatures. This behavior can be traced back to the known strong sensitivity of solubility of Cu in α -Fe, where Cu is not soluble at low temperatures (in the FM state), but becomes weakly soluble at high temperatures close to and above the transition to the PM state [41].

Furthermore, using polyhedral template matching[44] on the dislocation structure, we have identified that the three sites directly surrounding the dislocation core resemble an fcc structure, while all other sites are clearly bcc, as was pointed out by Wang *et al.* [45].

Inspired by these observations, we have checked the linear correlation between the core segregation energy and the difference in solution energies between fcc and bcc structures,

$$\Delta E_{\text{sol}} = E_{\text{sol}}^{(\text{fcc})}(\text{X} \rightarrow \text{Fe}) - E_{\text{sol}}^{(\text{bcc})}(\text{X} \rightarrow \text{Fe}), \quad (1)$$

where the solubility for a given structure is calculated using EMTO-CPA as

$$E_{\text{sol}}(\text{X} \rightarrow \text{Fe}) = \left. \frac{\partial E(\text{X}_c\text{Fe}_{1-c})}{\partial c} \right|_{c \rightarrow 0}. \quad (2)$$

Given above definitions, a model describing segregation trends can be written as

$$E_{\text{seg}} = a\Delta E_{\text{sol}} + E_0, \quad (3)$$

where parameters a and E_0 are determined by performing a least-squares fit on all data, for all elements, and for both FM and PM states.

Values obtained from the model presented in Fig. 5 show remarkable similarity to the true segregation energies for both magnetic states. Importantly, we can identify the same two distinct groups of elements as in Fig. 1: 1) Mn, Ni, and Cu, strongly attracted to the core in the FM state and weakly interacting in the PM state; 2) V, Cr, and Co, whose interaction with the core is weak in both magnetic states. These results indicate that the impurity-dislocation interaction for $3d$ elements is affected not only by magnetic effects, but also by coordination effects of at the dislocation core. This suggests the possibility of predicting trends in the segregation energies by considering solution energy differences of simple structures.

To conclude, we have investigated the effect of the ferromagnetic-to-paramagnetic transition in bulk α -Fe on the interaction of $3d$ -metal impurities with a screw dislocation. We have found that the magnetic state has a strong impact on the behavior of impurities, leading to the inversion of the interaction for some of the elements (Co, Ni, Cu). Especially large changes are observed for Cu, exhibiting strong segregation to the dislocation core in the ferromagnetic state at low temperature, while becoming repulsive in the paramagnetic state at high temperatures. Furthermore, this crossover is accompanied by significant changes in the shape of the energy profile

in the vicinity of the core. Similar, but weaker behavior is observed for Ni and Mn. We have shown that the behavior of all impurities around a screw dislocation significantly correlates with the differences between the solution energies of fcc and bcc structures of respective elements. The observed behavior of impurities can have implications on the plasticity of Fe-based alloys, especially at temperatures around the Curie temperature, relevant for heat treatment.

F.M. would like to thank Y. Wang (PQI) and H. Xue (UTK) for discussions and hospitality during the stay at UTK and ORNL. This work was supported by the Forschungsförderungsgesellschaft (FFG) project No. 878968 “ADAMANT”, Austrian Science Fond (FWF) project No. 33491-N “ReCALL”, COMET program IC-

MPPE (project No 859480), and Austrian Marshall Plan Foundation The COMET program is supported by the Austrian Federal Ministries for Climate Action, Environment, Energy, Mobility, Innovation and Technology (BMK) and for Digital and Economic Affairs (BMDW), represented by the Austrian research funding association (FFG), and the federal states of Styria, Upper Austria and Tyrol. This research used resources of the Oak Ridge Leadership Computing Facility, which is a DOE Office of Science User Facility supported under Contract DE-AC05-00OR22725 and the Vienna Scientific Cluster (VSC-5). Some computations were enabled by resources provided by the National Academic Infrastructure for Supercomputing in Sweden (NAISS), partially funded by the Swedish Research Council through grant agreement no. 2022-06725.

-
- [1] J. W. Christian, *Metallurgical Transactions A* **14**, 1237 (1983).
- [2] Y. K. T. Suzuki and H. O. K. Kirchner, *Philosophical Magazine A* **79**, 1629 (1999), <https://doi.org/10.1080/01418619908210383>.
- [3] H. Lim, C. C. Battaile, J. D. Carroll, B. L. Boyce, and C. R. Weinberger, *Journal of the Mechanics and Physics of Solids* **74**, 80 (2015).
- [4] C. R. Weinberger, B. L. Boyce, and C. C. Battaile, *International materials reviews* **58**, 296 (2013).
- [5] R. C. P. V. Vitek and D. K. Bowen, *The Philosophical Magazine: A Journal of Theoretical Experimental and Applied Physics* **21**, 1049 (1970), <https://doi.org/10.1080/14786437008238490>.
- [6] J. Bassani, K. Ito, and V. Vitek, *Materials Science and Engineering: A* **319-321**, 97 (2001).
- [7] L. Romaner, C. Ambrosch-Draxl, and R. Pippan, *Phys. Rev. Lett.* **104**, 195503 (2010).
- [8] V. R. L. Romaner and R. Pippan, *Philosophical Magazine Letters* **94**, 334 (2014).
- [9] H. Li, C. Draxl, S. Wurstler, R. Pippan, and L. Romaner, *Phys. Rev. B* **95**, 094114 (2017).
- [10] K. Obadrakh, G. Samolyuk, D. Nicholson, Y. Osetsky, R. E. Stoller, and G. M. Stocks, *Acta Materialia* **121** (2016), 10.1016/j.actamat.2016.08.074.
- [11] L. Casillas-Trujillo and B. Alling, *Journal of Applied Physics* **133** (2023).
- [12] H. K. D. H. Bhadeshia and R. W. K. Honeycombe, *Steels: microstructure and properties* (Butterworth-Heinemann, 2017).
- [13] L. Dezerald, L. Ventelon, E. Clouet, C. Denoual, D. Rodney, and F. Willaime, *Physical Review B* **89**, 024104 (2014).
- [14] E. Clouet, S. Garruchet, H. Nguyen, M. Perez, and C. S. Becquart, *Acta Materialia* **56**, 3450 (2008).
- [15] L. Ventelon, F. Willaime, E. Clouet, and D. Rodney, *Acta Materialia* **61**, 3973 (2013).
- [16] L. Casillas-Trujillo, D. Gambino, L. Ventelon, and B. Alling, *Physical Review B* **102**, 094420 (2020).
- [17] F. Maresca and W. A. Curtin, *Acta Materialia* **182**, 144 (2020).
- [18] S. Rao, C. Woodward, B. Akdim, O. Senkov, and D. Miracle, *Acta Materialia* **209**, 116758 (2021).
- [19] C. R. LaRosa, M. Shih, C. Varvenne, and M. Ghazisaeidi, *Materials Characterization* **151**, 310 (2019).
- [20] G. Kresse and J. Hafner, *Phys. Rev. B* **47**, 558 (1993).
- [21] G. Kresse and J. Furthmüller, *Phys. Rev. B* **54**, 11169 (1996).
- [22] G. Kresse and J. Furthmüller, *Nato. Sc. S. Ss. Iii. C. S.* **6**, 15 (1996).
- [23] G. Kresse and J. Hafner, *J. Phys. Condens. Matter* **6**, 8245 (1994).
- [24] G. Kresse and D. Joubert, *Phys. Rev. B* **59**, 1758 (1999).
- [25] L. Vitos, *Phys. Rev. B* **64**, 014107 (2001).
- [26] L. Vitos, J. Kollár, and H. L. Skriver, *Phys. Rev. B* **55**, 13521 (1997).
- [27] A. V. Ruban and M. Dehghani, *Physical Review B* **94**, 104111 (2016).
- [28] I. A. Abrikosov, S. I. Simak, B. Johansson, A. V. Ruban, and H. L. Skriver, *Phys. Rev. B* **56**, 9319 (1997).
- [29] O. E. Peil, A. V. Ruban, and B. Johansson, *Phys. Rev. B* **85**, 165140 (2012).
- [30] Y. Wang, G. M. Stocks, W. Shelton, D. Nicholson, Z. Szotek, and W. Temmerman, *Physical review letters* **75**, 2867 (1995).
- [31] M. Eisenbach, J. Larkin, J. Lutjens, S. Rennich, and J. H. Rogers, *Computer Physics Communications* **211**, 2 (2017).
- [32] D. M. Rogers, *Journal of Molecular Graphics and Modelling* **68**, 197 (2016).
- [33] A. V. Ruban and V. I. Razumovskiy, *Physical Review B—Condensed Matter and Materials Physics* **85**, 174407 (2012).
- [34] W. Cai, V. V. Bulatov, J. Chang, J. Li, and S. Yip, *Philosophical Magazine* **83**, 539 (2003), <https://doi.org/10.1080/0141861021000051109>.
- [35] J. P. Perdew and Y. Wang, *Phys. Rev. B* **45**, 13244 (1992).
- [36] J. P. Perdew, K. Burke, and M. Ernzerhof, *Physical review letters* **77**, 3865 (1996).
- [37] Z. Wu and R. E. Cohen, *Physical Review B* **73**, 235116 (2006).
- [38] H. Park, A. J. Millis, and C. A. Marianetti, *Physical*

- Review B **92**, 035146 (2015).
- [39] F. Moitzi, L. Romaner, A. V. Ruban, and O. E. Peil, *Phys. Rev. Mater.* **6**, 103602 (2022).
- [40] V. I. Razumovskiy and L. Romaner, “Spin-wave method calculations confirmed the stability of the easy-core configuration in the paramagnetic state,” Private Communication (2017), personal communication.
- [41] O. I. Gorbatov, I. K. Razumov, Y. N. Gornostyrev, V. I. Razumovskiy, P. A. Korzhavyi, and A. V. Ruban, *Phys. Rev. B* **88**, 174113 (2013).
- [42] Z. S. Basinski, W. Hume-Rothery, and A. Sutton, *Proceedings of the Royal Society of London. Series A. Mathematical and Physical Sciences* **229**, 459 (1955).
- [43] J. Crangle and G. Goodman, *Proceedings of the Royal Society of London. A. Mathematical and Physical Sciences* **321**, 477 (1971).
- [44] P. M. Larsen, S. Schmidt, and J. Schiøtz, *Model. Simul. Mater. Sc.* **24**, 055007 (2016).
- [45] R. Wang, L. Zhu, S. Pattamatta, D. J. Srolovitz, and Z. Wu, *Materials Today* **79**, 36 (2024).